DATASET BRIEF

An interactome map of the nucleocapsid protein from a highly pathogenic North American porcine reproductive and respiratory syndrome virus strain generated using SILAC-based quantitative proteomics

Stefanie S. Jourdan[1], Fernando Osorio[2] and Julian A. Hiscox[1]

[1] Institute of Molecular and Cellular Biology, Faculty of Biological Sciences, and Astbury Centre for Structural Molecular Biology, University of Leeds, Leeds, UK
[2] School of Veterinary and Biomedical Sciences, University of Nebraska-Lincoln, Lincoln, NE, USA

Received: September 7, 2011
Revised: December 8, 2011
Accepted: January 16, 2012

Positive strand RNA viruses replicate in the cytoplasm of an infected cell and encode nucleocapsid proteins. These proteins function to promote encapsidation of the RNA genome and virus particle assembly as well as playing potential roles in viral RNA synthesis. Nucleocapsid proteins can also associate with cellular proteins and signaling cascades. The arterivirus nucleocapsid (N) protein is no exception and localizes to both the cytoplasm and the nucleolus in virus-infected cells. This study generated an interactome map of the N protein from a highly virulent North American strain of porcine reproductive and respiratory syndrome virus (PRRSV). This is a major pathogen of swine resulting in significant morbidity and mortality. Crucial to the study was the use of SILAC coupled to affinity purification using GFP-traps and LC-MS/MS. This approach has not been applied before to the investigation of host/viral protein interactomes and this study revealed that the PRRSV N protein interacts with the host cell protein synthesis machinery especially at the level of translation initiation as well as with the RNA post-transcriptional modification machinery. Applications of the dataset can include studies of virus/host interactions and the design of live attenuated recombinant vaccines.

Keywords:
Bioinformatics / MASCOT / Microbiology / Multiprotein complex / Stable isotope labelling

Porcine reproductive and respiratory syndrome virus (PRRSV) causes reproductive failure in pregnant sows, a high mortality in piglets and respiratory disease in pigs of any age [1]. The spread of PRRSV can theoretically be controlled by vaccination. Although inactivated vaccines have been used to attempt to contain the disease, live attenuated vaccines are the only type capable of establishing protective immunity [2]. However, currently available live vaccine strains are unstable and sometimes revert to virulent phenotypes in vaccinated animals. Emerging research suggests that live vaccines based on recombinant viruses with selected multiple attenuating mutations offer the best potential for future vaccine efforts. Due to the high losses in production resulting from PRRSV infection, the virus is of great economic importance. PRRSV belongs to the family of arteriviruses that are grouped together with the Corona- and Toroviruses into the order *Nidovirales*. During arterivirus (and coronavirus) infection, one of the most abundant viral proteins within the cell is the N protein that plays essential roles in the virus life cycle including encapsidation of the viral RNA [3]. Although these viruses replicate in the cytoplasm, the N protein has been

Correspondence: Dr. Julian A. Hiscox, Room 8.58, Garstang Building, Institute of Molecular and Cellular Biology, Faculty of Biological Sciences, University of Leeds, UK
E-mail: j.a.hiscox@leeds.ac.uk
Fax: +44-113-343-5638

Abbreviations: EGFP, enhanced GFP; **GFP**, green fluorescent protein; **N protein**, nucleocapsid protein; **PABP**, poly(A) binding protein; **PRRSV**, porcine reproductive and respiratory syndrome virus

observed to localize to the nucleolus in a wide range of corona and arteriviruses [4–8].

Nidovirus proteins have also been reported to interact with cellular proteins and signaling cascades. For PRRSV predominant amongst these is the potential involvement of N protein in modulation of host cell function and recruiting cellular factors to facilitate virus replication [9]. Several amino acid motifs on the N protein have been identified that are involved in the cytoplasmic/nuclear/nucleolar trafficking of the protein and also interactions with cellular proteins [10–12]. N protein has been shown to interact with importin-α and importin-β [12], the nucleolar protein fibrillarin, [13] and several others [9].

Given the importance of the N protein in the life cycles of arteriviruses and the role of these viruses in health and food security, we decided to generate a cellular interactome map of the arterivirus N protein using enhanced green fluorescent protein (EGFP)-trap technology coupled to SILAC to help distinguish background binding from potentially specific interactions [14]. LC-MS/MS was used to identify and quantify proteins, and binding to selected cellular proteins was validated using Western blot in separate technical non-labeled biological replicates. The potential use of the dataset was then demonstrated. The EGFP-N protein fusion approach was taken in order to fully utilize the high affinity of the GFP-trap (Chromotek), which consists of a single domain anti-GFP antibody conjugated to an agarose bead matrix. This approach was also taken over selectively immuno-precipitating N protein from PRRSV-infected cells as we wanted to examine the specific interaction of N protein with cellular components. In PPRSV infected cells, N protein may interact with other viral proteins which themselves will bind to cellular proteins.

In order to generate an N protein fused to EGFP, the PRRSV N gene was cloned upstream of the recombinant GFP (RGFP) gene from the genome of a pathogenic PRRSV template produced by a cDNA infectious clone derived from isolate NVSL #97-7895 [15]. Alanine subsitution mutants of N protein to illustrate applications of the dataset were generated in a yellow fluorescent protein (YFP)-background. For SILAC-assisted EGFP-Trap® pull-downs 293-T cells were grown in stable isotope labeled growth media containing "light" (R0K0) or "heavy" (R10K8) arginine and lysine for a period of 2 weeks (>5 cell divisions) prior to harvest. For both light and heavy labeled cells, four 10-cm dishes were seeded with 1.25×10^6 cells each 24 h prior to transfection of the dishes with 10-μg plasmid DNA coding for EGFP or N-EGFP, respectively. Twenty-four hours post transfection cells were harvested and counted and equal numbers of cells were used to prepare lysates for the EGFP-Trap. After processing equal volumes, labeled samples were mixed and analyzed by LC-MS/MS with detailed methods presented previously [16, 17]. Ingenuity pathway analysis (IPA) was used to analyze and interrogate the cellular protein datasets and to group proteins into similar functional classes.

N-EGFP fusion protein localized to the nucleolus and the cytoplasm in 293-T cells (Supporting Information Fig. 1) was identical to the pattern found for this protein in Marc145 cells [6, 13] and other cell types, such as Vero cells [18]. GFP-Trap® beads were used to carry out pull-down experiments using cell lysates from cells expressing N-EGFP or EGFP. Quantitative proteomic analysis using LC-MS/MS of the cellular proteins was eluted off the beads identified 224 cellular proteins (Supporting Information Table S1). Confidence in protein identification was considered high if the PEP (posterior error probability) score was close to zero. In several cases very similar proteins belonging to the same family, e.g. PABP1 and PABPC4 may be assigned to a similar set of peptides and this information is presented in Supporting Information Table S1 (columns A and B). However, use of biological replicates and specific antibodies can help distinguish between these proteins (see below). Raw data was deposited with the PRoteomics IDEntifications database (PRIDE) [19] using the PRIDE converter [20]. This dataset was also deposited with the IMEx molecular interaction database through IntAct [21, 22] and assigned the identifier IM-16317.

Fifty-six cellular proteins were identified and quantified by two or more peptides and were enriched two-fold or more in the N-EGFP fraction compared to the EGFP fraction. These proteins were grouped into categories with similar functions (Table 1) and used in further analysis to validate the dataset and demonstrate its application. Apart from background binding, a number of these proteins may form dynamic or weak interactions with N protein, and hence not be enriched in the N-EGFP pull-down compared to the EGFP pull-down control (Supporting Information Table S1). Present amongst these are importin-5 (0.76), nucleolin (0.74), and ribosomal proteins that have previously been shown to interact with arterivirus and/or coronavirus N proteins [9] (also see Table 1).

Bioinformatic analysis of the dataset using IPA indicated that N-EGFP associated with proteins involved a number of different molecular and cellular functions including: RNA post-transcriptional modification (splicing) (24 molecules, p-value $1.41 \times 10^{-28} - 4.19 \times 10^{-2}$), protein synthesis (11 molecules, p-value $2.09 \times 10^{-8} - 3.51 \times 10^{-2}$), RNA trafficking (8 molecules, p-value $1.64 \times 10^{-7} - 2.12 \times 10^{-2}$), and gene expression (22 molecules, p-value $7.75 \times 10^{-6} - 4.53 \times 10^{-2}$) (Fig. 1A). Many of these proteins are shared between the different functions and can be linked by known protein–protein interactions (Fig. 1B).

To confirm the LC-MS/MS data, pull-downs were repeated in a separate experiment in the absence of label and were analyzed by Western blot using antibodies specific against a selection of hits representing different functional classes focused on translation and splicing, e.g. poly(A) binding protein (PABP), inducible PABP (iPABP), translation initiation factor 4E (eIF4E), hnRNPA1, and NONO (Fig.2A). These were selected on the basis of interest but also representing

Table 1. Proteins identified in the N-EGFP Trap and differentiated from background EGFP binding using SILAC

Protein ID	Gene name	Protein name	N-EGFP / EGFP	Pep.	Seq. cov. (%)	PEP	Notes
Translation							
IPI00555747.1	PABPC4	Inducible polyadenylate-binding protein 1	17	30	41.5	0	Binds to the poly(A) tail
IPI00008524.1	PABPC1	Polyadenylate-binding protein 1	16	34	48.1	0	Binds to the poly(A) tail. Shown to bind to the 3′ untranslated region and polyA tail of coronavirus genomes [33, 34]
IPI00646377.1	EIF4G3	Eukaryotic translation initiation factor 4 gamma 3	8	4	2.5	6.7E-21	Involved in the recognition of the mRNA cap
IPI00873680.2	EIF4E	Eukaryotic translation initiation factor 4E	5	3	12.9	2.2E-12	Recognizes the mRNA cap and facilitates ribosome's binding by unwinding mRNA secondary structure
IPI00719752.1	EIF3B	Eukaryotic translation initiation factor 3 subunit B	4	11	14	3.3E-22	Part of the eIF-3 complex that facilitates recruitment of mRNA to the 43S pre-initiation complex for AUG recognition
IPI00646839.1	EIF3C	Eukaryotic translation initiation factor 3 subunit C	5	11	12.7	3.0 E-39	As above
IPI00465233.1	EIF3EIP	Eukaryotic translation initiation factor 3, subunit E interacting protein	5	3	6.6	7.4E-16	As above
IPI00871852.1	EIF4A1	ATP-dependent RNA helicase eIF4A-1	4	7	21.7	5.7E-31	Involved in cap recognition and binding of mRNA to the ribosome. Found in PRRSV virions [32]
IPI00412343.2	FMR1	Fragile X mental retardation 1 protein	2	3	4.9	0.0003	Repressor of translation, binds to the CAP
IPI00418313.3	ILF3	Interleukin enhancer-binding factor 3	2	13	16.3	3.7E-30	Translation inhibitory protein. Can complex with HNRNPs, nucleolin and other proteins
mRNA stability							
IPI00399170.1	UPF1	ATP-dependent helicase RENT1	4	20	22	6.8E-53	Degradation of mRNAs containing premature stop codons
IPI00784170.1	DHX36	DEAH box protein 36	2	6	7	3.3E-24	Degradation and deadenylation of mRNAs
IPI00479786.5	KHSRP	Far upstream element-binding protein 2	2	7	11.1	2.3E-35	Involved in mRNA trafficking, degradation of unstable mRNAs
IPI00301936.4	ELAVL1	ELAV-like protein 1	5	5	16.4	4.0E-14	Involved in mRNA stabilization, specifically to FOS and IL3 mRNAs
IPI00008557.5	IGF2BP1	Insulin-like growth factor 2 mRNA-binding protein 1	4	20	40.2	1.1E-87	mRNA trafficking and stability, can function in stress granules
IPI00658000.2	IGF2BP3	Insulin-like growth factor 2 mRNA-binding protein 3	3	12	25.9	4.6E-41	Role in mRNA stability binds to the 5′ UTR of IGF2 mRNA and the 3′ UTR of CD44 mRNA
IPI00797384.2	LARP4	La-related protein 4	2	3	2.8	6.1xE-19	Binds with poly(A) RNA and interacts with PABP. Can promote RNA stability
IPI00032355.3	PUM1	Pumilio homolog 1 (Drosophila)	2	2	2.1	0.014	Regulates translation and mRNA stability by binding the 3′ UTR of mRNA targets
Heterogeneous nuclear ribonucleoproteins							
Involved in mRNA export and splicing							
IPI00011274.3	HNRPDL	Heterogeneous nuclear ribonucleoprotein D-like	3	5	11.7	1.4E-18	Promotes transcriptional repression, binds to RNA molecules that contain AU-rich elements (AREs) found within the 3 UTRs of many cytokine mRNAs

Table 1. Continued

Protein ID	Gene name	Protein name	N-EGFP / EGFP	Pep.	Seq. cov.(%)	PEP	Notes
IPI00216746.1	HNRNPK	Heterogeneous nuclear ribonucleoprotein K	3	12	35.6	1.3E-87	Major pre-mRNA binding protein and has a high affinity for poly(C) sequences
IPI00479191.2	HNRNPH1	Heterogeneous nuclear ribonucleoprotein H	3	6	19.5	7.2E-69	Mediates pre-mRNA alternative splicing regulation
IPI00013877.2	HNRNPH3	Heterogeneous nuclear ribonucleoprotein H3	3	2	8.4	1.2E-09	Involved in splicing and heat shock-induced splicing arrest
IPI00396378.3	HNRNPA2B1	Heterogeneous nuclear ribonucleoproteins A2/B1	4	15	45	7.0E-74	Involved in pre-mRNA processing and found in the nucleolus. Interacts with the 3′ end of the coronavirus genome [34]
IPI00215965.2	HNRNPA1	Heterogeneous nuclear ribonucleoprotein A1	3	16	43	9.6E-113	May modulate splice sites selection and packaging of pre-mRNA into hnRNP particles. Interacts with the 3′ end of the coronavirus genome [34] and sites of transcription initiation [35, 36]. Binds to SARS-coronavirus N protein [37]. May regulate coronavirus RNA synthesis [38]
IPI00419373.1	HNRNPA3	Heterogeneous nuclear ribonucleoprotein A3	3	6	25.7	5.4E-34	Functions in trafficking RNA and pre-mRNA splicing
IPI00003881.5	HNRNPF	Heterogeneous nuclear ribonucleoprotein F	2	3	10.6	4.7E-43	Involved in pre-mRNA processing and regulation of alternative splicing events
IPI00011913.1	HNRNPA0	Heterogeneous nuclear ribonucleoprotein A0	2	4	17.7	1.7E-48	Component of ribonucleosomes
IPI00304692.1	RBMX	Heterogeneous nuclear ribonucleoprotein G	2	2	6.6	6.9E-07	Involved in pre-MRNA splicing
IPI00477313.3	HNRNPC	Heterogeneous nuclear ribonucleoproteins C1/C2	2	5	19.6	2.2E-48	Binds pre-mRNA and nucleates the assembly of 40S hnRNP particles
Splicing							
IPI00216613.1	SFPQ	Polypyrimidine tract-binding protein-associated-splicing factor	4	10	17.5	1.6E-86	Also termed SFPQ, interacts with NONO. DNA- and RNA binding protein, involved in several nuclear processes including splicesome formation
IPI00183626.8	PTBP1	Polypyrimidine tract-binding protein 1	4	11	26.8	4.1E-26	Involved in pre-mRNA splicing and binds to the polypyrimidine tract of introns. May promote RNA looping. Interacts with the 3′ end of the arterivirus genome [39]. Interacts with the 5′ end [40] and 3′ end of the coronavirus genome, and silencing resulted in a reduction in viral RNA synthesis [34]
IPI00215884.4	SRSF1	Splicing factor, arginine/serine-rich 1	4	6	29.8	3.5E-18	Involved in splicing
IPI00010204.1	SRSF3	Splicing factor, arginine/serine-rich 3	4	3	24.4	9.8E-11	Involved in splicing
IPI00000015.2	SRSF4	Splicing factor, arginine/serine-rich 4	3	2	3.2	3.8E-06	Involved in splicing
IPI00003377.1	SRSF7	Splicing factor, arginine/serine-rich 7	4	2	8.8	0.0001	Involved in splicing
IPI00304596.3	NONO	Non-POU domain-containing octamer-binding protein (NONO)	4	12	25.3	1.7E-57	Involved in pre-mRNA splicing

Table 1. Continued

Protein ID	Gene name	Protein name	N-EGFP / EGFP	Pep.	Seq. cov.(%)	PEP	Notes
IPI00011550.1	ZCCHC3	Zinc finger CCHC domain-containing protein 3	2	2	6.4	3.8E-05	May be involved in pre-mRNA splicing
IPI00643351.1	YBX1	Nuclease-sensitive element-binding protein 1	2	9	43	4.7E-115	Can determine splice site selection
IPI00294536.2	STRAP	Serine-threonine kinase receptor-associated protein	2	3	12.4	1.6E-10	Required for pre-mRNA splicing and formation of splicesomal snRNP in the cytoplasm
Dead/Deah RNA helicases							
Characterized by containing the conserved motif Asp-Glu-Ala-Asp (DEAD). Involved in alteration of RNA secondary structure from translation to splicing.							
IPI00293616.3	DDX3X	DEAD box protein 3	3	10	18.3	2.3E-120	ATP-dependent RNA helicase
IPI00017617.1	DDX5	DEAD box protein 5	3	14	23.8	3.2E-73	ATP-dependent RNA helicase found in the spliceosome C complex
IPI00844578.1	DHX9	DEAH box protein 9	2	32	29.8	1.4E-198	Unwinds RNA in a 3′ to 5′ direction. Promotes MYC mRNA stability
IPI00651653.1	DDX17	DEAD box protein 17	4	16	22.8	1.1E-72	ATP-dependent RNA helicase
IPI00411733.4	DHX30	DEAH box protein 30	2	13	12.8	2.3E-31	ATP-dependent RNA helicase, identified in a complex with TFAM and SSBP1
RNA binding							
IPI00260715.5	FUS	RNA-binding protein FUS	3	4	10.8	1.3E-19	Binds DNA and RNA
IPI00783271.1	LRPPRC	Leucine-rich PPR motif-containing protein, mitochondrial	3	12	11	4.7E-58	Binds to HNRPA1-associated poly(A) mRNAs, and also in mitochondria to polyA
IPI00185919.3	LARP1	La-related protein 1	12	28	31.5	4.8E-132	Contains a La motif, involved in RNA binding. Co-localizes with P bodies, which function in RNA degradation
IPI00827634.2	LARP5	La-related protein 5	7	3	3.9	1.4E-05	RNA binding
Other proteins							
IPI00444452.3	MOV10	Putative helicase MOV-10	3	3	3.6	5.9E-11	Probable helicase. Part of the RNA-induced silencing complex (RISC)
IPI00641950.3	GNB2L1	Guanine nucleotide-binding protein subunit beta-2-like 1	4	13	50.1	3.2E-97	Anchors activated PKC to the cytoskeleton, acts as a platform for SRC activation or inactivation
IPI00789551.1	MATR3	Matrin-3	3	6	9.7	1.1E-23	Associates with NONO and involved in the nuclear retention of defective RNAs
IPI00083708.3	PRRC2C	BAT2 domain-containing protein 1	3	2	0.8	4.9E-07	May function in the regulation of gene expression
IPI00216689.2	PCBP2	Poly (rC)-binding protein 2	2	6	23.2	1.6E-23	Negatively regulates cellular antiviral responses mediated by MAVS signaling
IPI00005198.2	ILF2	Interleukin enhancer-binding factor 2	2	3	10.3	1.5E-10	Transcription factor
IPI00879750.1	SNRPD3	Small nuclear ribonucleoprotein Sm D3	2	3	22.9	2.2E-15	Part of the U7 snRNP complex, identified in the spliceosome C complex
IPI00456363.1	ATXN2L	Ataxin-2-like protein	2	3	2.8	4.1E-12	Unknown function

Only proteins showing a binding ratio greater than two or more and identified by two or more peptides are shown. Detailed are the protein ID, protein name, binding ratio, number of individual peptides used to identify the protein (pep.), the percentage sequence coverage on the protein this represents (Seq. Cov. [%]), the posterior error probability (PEP) that is used to calculate the false discovery rate and brief notes on the protein function (generally taken from Uniprot). For interpretation, proteins are grouped into functional categories and/or classes. Notes refer to actual/potential protein function and also indicate where an interaction has been shown to occur previously with PRRSV, arteriviruses, or related coronaviruses.

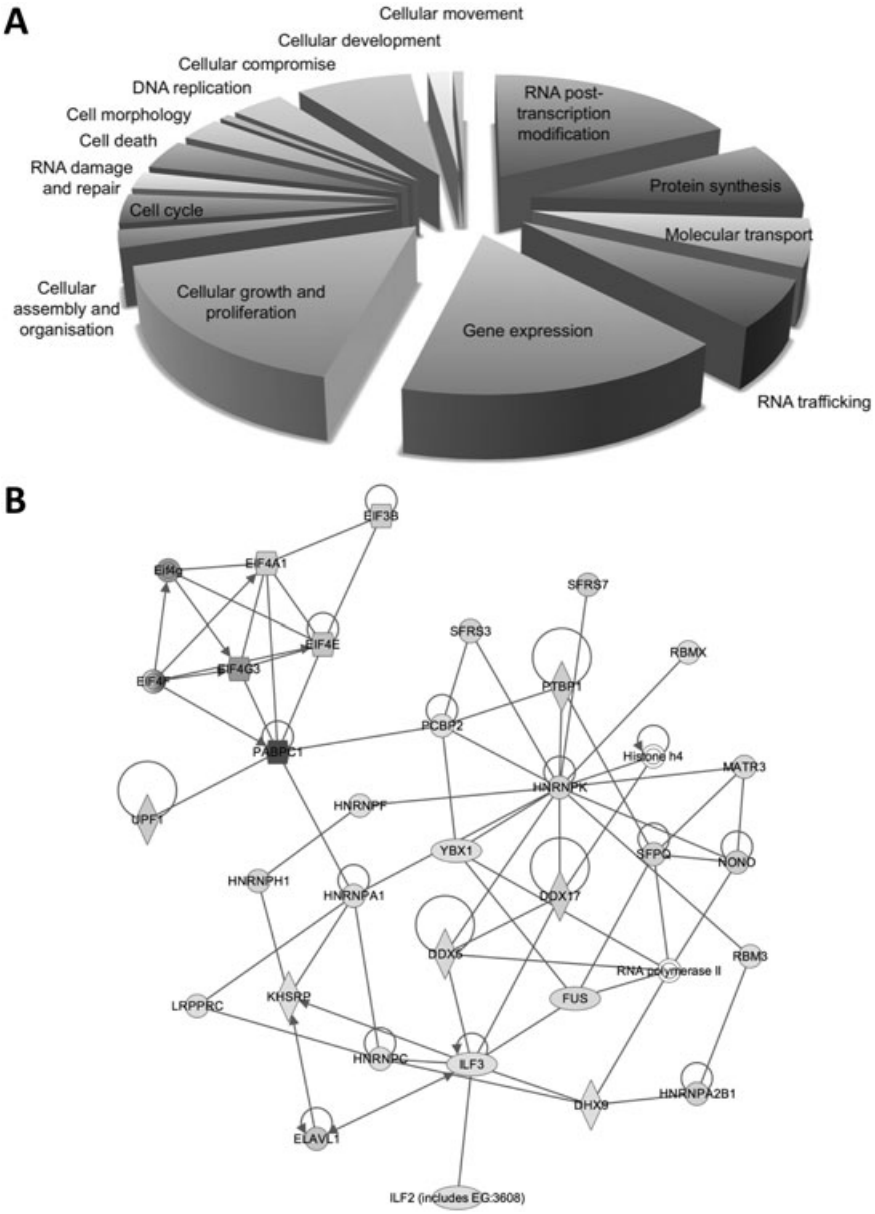

Figure 1. Bioinformatic analysis using Ingenuity Pathway Analysis of the PRRSV interactome dataset detailed in Table 1. (A) Pie chart showing the interactome classified according to cellular and molecular function. (B) Interactome map from data uploaded to Ingenuity Pathway Analysis (IPA) of proteins associated with PRRSV N protein identified in the SILAC pull-downs focusing on proteins associated with protein synthesis and RNA post-transcriptional modification. The degree of shading represents abundance above EGFP-control in the N-EGFP pull-down. The shape denotes the molecular class of the protein and solid line indicates a direct molecular interaction. A line that exists as a circular arrow indicates that the molecule can also act upon itself. Further information is provided in Supporting Information Figure S3.

proteins identified from a large and small number of peptides and ratios, e.g. iPABP (30 peptides and 17-fold enhanced) and eiF4E (3 peptides and 5-fold enhanced). They indicated that N-EGFP interacted with protein components of the translation initiation complex (Fig. 2B). The interaction of N protein with the selected cellular proteins was also assessed by disulfide reduction in the pull down reactions. N protein has been reported to multimerize, particularly into dimers [23] with one mechanism through the role of potential disulfide linkages [24, 25]. Therefore disruption of disulfide bridge formation would give an indication of whether binding to the cellular protein required multimeric N protein. No difference between the presence and absence of DTT was observed with any of the selected protein, apart from eIF4E, which appeared to bind less well to the N protein in the presence of DTT (Fig. 2A).

Given the role of the N protein in cytoplasmic/nuclear/nucleolar trafficking and previous studies showing the importance of some of these identified cellular proteins (that are found in the nucleus) in the related coronavirus biology (Table 1), it is tempting to speculate that the N protein maybe recruiting nuclear proteins to facilitate virus biology. Knowledge of N/cellular protein interactions can also be used to generate live recombinant vaccines based on attenuating mutations. The use of reverse genetics in PRRSV [15, 26] and the introduction of attenuating mutations [27, 28], including the N gene [10, 11], is a clearly established strategy for investigating PRRSV

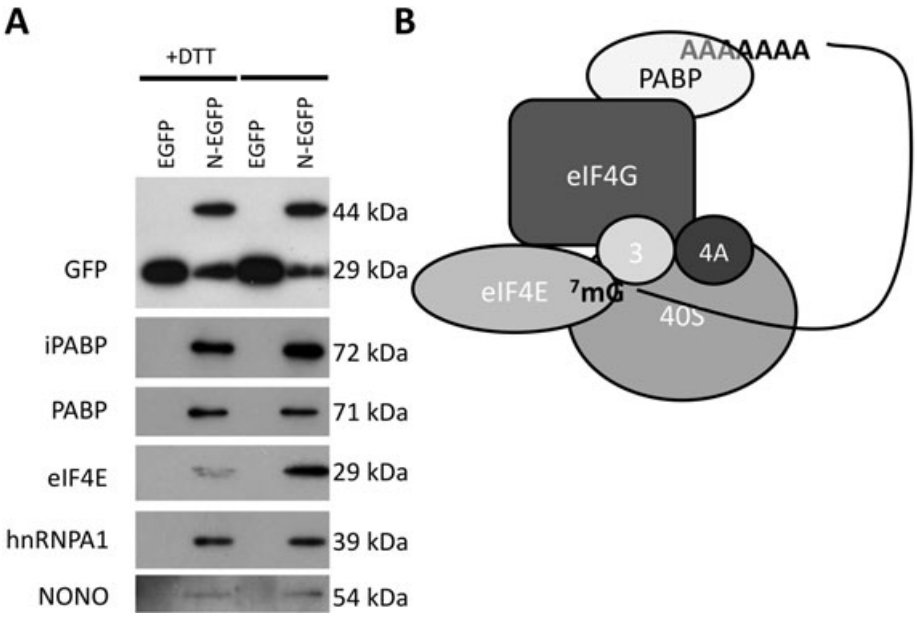

Figure 2. Validation of MS data. (A) Western blots were carried out on the bound fraction from cell lysates containing either EGFP or N-EGFP. Lysates were prepared, or with the addition or absence of DTT to a final concentration of 2 mM (+DTT). In the case of pull-downs carried out under reducing conditions (+DTT) also the dilution and wash buffer contained 2 mM DTT. (B) Schematic of the cap-dependent translation initiation complex depicting an RNA (black line) with its poly(A) tail and its 7-methylguanosine cap (^{7}mG). Shown in complex with the RNA are the PABP that binds to the mRNA's poly(A) tail as well as to the initiation factor 4G. As eIF4G binds to eIF4E which interacts with the ^{7}mG, circularization of the mRNA is achieved. eIF3 and 4A interact with eIF4G allowing for the recruitment of the 40S ribosomal subunit.

biology and generating potential live recombinant vaccines. In this case, the N interactome dataset can be mined in order to determine what cellular proteins are important for N-protein function during virus replication. The binding site(s) on the N protein to a selected cellular protein can be determined and then mutagenesis used to knock out this function on the N protein. These mutations can then be introduced into the N gene in the context of the virus, using reverse genetics, and appropriate virological assays performed to assess the impact on virus replication and growth. Mutations in N protein that result in a reduction of virus replication and growth can be considered attenuating, and provide potential for a live attenuated recombinant vaccine, which is crucial for controlling PRRSV in the field [2, 9, 29]. To illustrate this use of the dataset, a series of N-protein mutants containing sequential alanine substitutions were expressed in cells as YFP-fusion proteins to map the PABP/iPABP binding site(s) (Supporting Information Fig. 2).

This dataset can also be compared to other proteomic approaches that have been applied to the study of PRRSV interactions with the host cell and virus particles, which include changes in the abundance of proteins involved in translation [30–32]. To our knowledge, this is the first application of SILAC coupled to GFP-Trap pull-downs for the analysis of a viral protein and mapping an interactome. Here we demonstrated the PRRSV N protein associated with numerous cellular proteins, predominately those involved in forming the translation initiation complex and splicing.

Raw data was deposited to PRIDE using the PRIDE converter (contact authors for accession numbers), and also deposited with the IMExmolecular interaction database through IntAct (identifier IM-16317).

This work was funded by a Leverhulme Trust Research Fellowship to J.A.H., and developed from a National Pork Board project grant awarded to F.A.O. and J.A.H. We would like to thank Sandra Orchard at the European Bioinformatics Institute for help and guidance.

The authors have declared no conflict of interest.

References

[1] Meulenberg, J. J. M., Hulst, M. M., de Meijer, E. J., Moonen, P. L. J. M. et al., Lelystad virus, the causative agent of porcine epidemic abortion and respiratory syndrome (PEARS), is related to LDV and EAV. *Virology* 1993, *192*, 62–72.

[2] Zuckermann, F. A., Garcia, E. A., Luque, I. D., Christopher-Hennings, J. et al., Assessment of the efficacy of commercial porcine reproductive and respiratory syndrome virus (PRRSV) vaccines based on measurement of serologic response, frequency of gamma-IFN-producing cells and virological parameters of protection upon challenge. *Vet. Microbiol.* 2007, *123*, 69–85.

[3] Spilman, M. S., Welbon, C., Nelson, E., Dokland, T., Cryo-electron tomography of porcine reproductive and respiratory syndrome virus: organization of the nucleocapsid. *J. Gen. Virol.* 2009, *90*, 527–535.

[4] Wurm, T., Chen, H., Hodgson, T., Britton, P. et al., Localization to the nucleolus is a common feature of coronavirus nucleoproteins, and the protein may disrupt host cell division. *J. Virol.* 2001, *75*, 9345–9356.

[5] Tijms, M. A., van der Meer, Y., Snijder, E. J., Nuclear localization of non-structural protein 1 and nucleocapsid protein of equine arteritis virus. *J. Gen. Virol.* 2002, *83*, 795–800.

[6] Rowland, R. R., Kervin, R., Kuckleburg, C., Sperlich, A., Benfield, D. A., The localization of porcine reproductive and respiratory syndrome virus nucleocapsid protein to the nucleolus of infected cells and identification of a potential nucleolar localization signal sequence. *Virus Res.* 1999, *64*, 1–12.

[7] Hiscox, J. A., Wurm, T., Wilson, L., Britton, P. et al., The coronavirus infectious bronchitis virus nucleoprotein localizes to the nucleolus. *J. Virol.* 2001, *75*, 506–512.

[8] Emmott, E., Dove, B. K., Howell, G., Chappell, L. A. et al., Viral nucleolar localisation signals determine dynamic trafficking within the nucleolus. *Virology* 2008, *380*, 191–202.

[9] Yoo, D., Song, C., Sun, Y., Du, Y. et al., Modulation of host cell responses and evasion strategies for porcine reproductive and respiratory syndrome virus. *Virus Res.* 2010, *154*, 48–60.

[10] Lee, C., Hodgins, D., Calvert, J. G., Welch, S. K. et al., Mutations within the nuclear localization signal of the porcine reproductive and respiratory syndrome virus nucleocapsid protein attenuate virus replication. *Virology* 2006, *346*, 238–250.

[11] Pei, Y., Hodgins, D. C., Lee, C., Calvert, J. G. et al., Functional mapping of the porcine reproductive and respiratory syndrome virus capsid protein nuclear localization signal and its pathogenic association. *Virus Res.* 2008, *135*, 107–114.

[12] Rowland, R. R. R., Schneider, P., Fang, Y., Wootton, S. et al., Peptide domains involved in the localization of the porcine reproductive and respiratory syndrome virus nucleocapsid protein to the nucleolus. *Virology* 2003, *316*, 135–145.

[13] Yoo, D., Wootton, S. K., Li, G., Song, C., Rowland, R. R., Colocalization and interaction of the porcine arterivirus nucleocapsid protein with the small nucleolar RNA-associated protein fibrillarin. *J. Virol.* 2003, *77*, 12 173–12 183.

[14] Trinkle-Mulcahy, L., Boulon, S., Lam, Y. W., Urcia, R. et al., Identifying specific protein interaction partners using quantitative mass spectrometry and bead proteomes. *J. Cell Biol.* 2008, *183*, 223–239.

[15] Truong, H. M., Lu Z., Kutish, G. F., Galeota J. et al., A highly pathogenic porcine reproductive and respiratory syndrome virus generated from an infectious cDNA clone retains the in vivo virulence and transmissibility properties of the parental virus. *Virology* 2004, *325*, 308–319.

[16] Munday, D. C., Emmott E., Surtees R., Lardeau, C. H. et al., Quantitative proteomic analysis of A549 cells infected with human respiratory syncytial virus. *Mol. Cell. Proteomics* 2010, *9*, 2438–2459.

[17] Emmott E., Rodgers, M. A., Macdonald A., McCrory S. et al., Quantitative proteomics using stable isotope labeling with amino acids in cell culture reveals changes in the cytoplasmic, nuclear, and nucleolar proteomes in vero cells infected with the coronavirus infectious bronchitis virus. *Mol. Cell Proteomics* 2010, *9*, 1920–1936.

[18] You, J. H., Howell G., Pattnaik, A. K., Osorio, F. A., Hiscox, J. A., A model for the dynamic nuclear/nucleolar/cytoplasmic trafficking of the porcine reproductive and respiratory syndrome virus (PRRSV) nucleocapsid protein based on live cell imaging. *Virology* 2008, *378*, 34–47.

[19] Vizcaino, J. A., Cote R., Reisinger F., Foster, J. M. et al., A guide to the Proteomics Identifications Database proteomics data repository. *Proteomics* 2009, *9*, 4276–4283.

[20] Barsnes, H., Vizcaino, J. A., Eidhammer, I., Martens, L., PRIDE Converter: making proteomics data-sharing easy. *Nat. Biotechnol.* 2009, *27*, 598–599.

[21] Kerrien S., Alam-Faruque Y., Aranda B., Bancarz I. et al., IntAct–open source resource for molecular interaction data. *Nucleic Acids Res.* 2007, *35*, D561–D565.

[22] Kerrien S., Aranda B., Breuza L., Bridge A. et al., The IntAct molecular interaction database in 2012. *Nucleic Acids Res.* 2012, *40*, D841–D846.

[23] Doan, D. N., Dokland T., Structure of the nucleocapsid protein of porcine reproductive and respiratory syndrome virus. *Structure* 2003, *11*, 1445–1451.

[24] Wootton, S. K., Yoo D., Homo-oligomerization of the porcine reproductive and respiratory syndrome virus nucleocapsid protein and the role of disulfide linkages. *J. Virol.* 2003, *77*, 4546–4557.

[25] Lee C., Calvert, J. G., Welch, S. K., Yoo D., A DNA-launched reverse genetics system for porcine reproductive and respiratory syndrome virus reveals that homodimerization of the nucleocapsid protein is essential for virus infectivity. *Virology* 2005, *331*, 47–62.

[26] Kwon B., Ansari, I. H., Osorio, F. A., Pattnaik, A. K., Infectious clone-derived viruses from virulent and vaccine strains of porcine reproductive and respiratory syndrome virus mimic biological properties of their parental viruses in a pregnant sow model. *Vaccine* 2006, *24*, 7071–7080.

[27] Kwon B., Ansari, I. H., Pattnaik, A. K., Osorio, F. A., Identification of virulence determinants of porcine reproductive and respiratory syndrome virus through construction of chimeric clones. *Virology* 2008, *380*, 371–378.

[28] Wang Y., Liang Y., Han J., Burkhart, K. M. et al., Attenuation of porcine reproductive and respiratory syndrome virus strain MN184 using chimeric construction with vaccine sequence. *Virology* 2008, *371*, 418–429.

[29] Huang, Y. W., Meng, X. J., Novel strategies and approaches to develop the next generation of vaccines against porcine reproductive and respiratory syndrome virus (PRRSV). *Virus Res.* 2010, *154*, 141–149.

[30] Zhang H., Guo X., Ge X., Chen Y. et al., Changes in the cellular proteins of pulmonary alveolar macrophage infected with porcine reproductive and respiratory syndrome virus by proteomics analysis. *J. Proteome. Res.* 2009, *8*, 3091–3097.

[31] Xiao S., Wang Q., Jia J., Cong P. et al., Proteome changes of lungs artificially infected with H-PRRSV and N-PRRSV by two-dimensional fluorescence difference gel electrophoresis. *Virol. J.* 2010, *7*, 107.

[32] Zhang C., Xue C., Li Y., Kong Q. et al., Profiling of cellular proteins in porcine reproductive and respiratory syndrome virus virions by proteomics analysis. *Virol. J.* 2010, *7*, 242.

[33] Spagnolo, J. F., Hogue, B. G., Host protein interactions with the 3′ end of bovine coronavirus RNA and the requirement of the poly(A) tail for coronavirus defective genome replication. *J. Virol.* 2000, *74*, 5053–5065.

[34] Galan C., Sola I., Nogales A., Thomas B. et al., Host cell proteins interacting with the 3′ end of TGEV coronavirus genome influence virus replication. *Virology* 2009, *391*, 304–314.

[35] Li, H. P., Zhang, X., Duncan, R., Comai, L., Lai, M. M., Heterogeneous nuclear ribonucleoprotein A1 binds to the transcription-regulatory region of mouse hepatitis virus RNA. *Proc. Natl. Acad. Sci. USA* 1997, *94*, 9544–9549.

[36] Zhang, X. M., Li, H. P., Xue, W. M., Lai, M. M. C., Formation of a ribonucleoprotein complex of mouse hepatitis virus involving heterogeneous nuclear ribonucleoprotein A1 and transcription-regulatory elements of viral RNA. *Virology* 1999, *264*, 115–124.

[37] Luo, H., Chen, Q., Chen, J., Chen, K. et al., The nucleocapsid protein of SARS coronavirus has a high binding affinity to the human cellular heterogeneous nuclear ribonucleoprotein A1. *FEBS Lett.* 2005, *579*, 2623–2628.

[38] Shi, S. T., Huang P., Li, H. P., Lai, M. M. C., Heterogeneous nuclear ribonucleoprotein A1 regulates RNA synthesis of a cytoplasmic virus. *EMBO J.* 2000, *19*, 4701–4711.

[39] Maines, T. R., Young, M., Dinh, N. N., Brinton, M. A., Two cellular proteins that interact with a stem loop in the simian hemorrhagic fever virus 3′(+)NCR RNA. *Virus Res.* 2005, *109*, 109–124.

[40] Li, H. P., Huang, P. Y., Park, S. M., Lai, M. M. C., Polypyrimidine tract-binding protein binds to the leader RNA of mouse hepatitis virus and serves as a regulator of viral transcription. *J. Virol.* 1999, *73*, 772–777.

